Experimental Study of the Dynamics of Front Propagation in the $Co(OH)_2/NH_4OH$ Liesegang System Using Spectrophotometry

Hazar Batlouni and Mazen Al-Ghoul*

Department of Chemistry, American University of Beirut, P.O. Box 11-0236, 1107 2020 Riad El Solh, Beirut, Lebanon

Received: April 10, 2008; Revised Manuscript Received: May 26, 2008

In this paper we study the temporal dynamics of the $Co(OH)_2/NH_4OH$ Liesegang system with redissolution by complex formation with ammonia using UV−vis spectrophotometry with a special setup. The formation of precipitate bands is accompanied with band redissolution at the top, and because of such precipitation−redissoultion dynamics, the bands appear as a propagating wave. The spectrophotometric technique developed in this study allows us to study at the kinetics of formation of the bands and their redissolution in great details. The formation, growth, and dissolution of multiple bands are monitored by the time evolution of the absorbance. It was found that the individual band formation is sudden and takes between 15 min to half an hour to form before the next band appears. The speed of formation of bands was different for different bands and the maxima of these speeds fit a Gaussian curve. The content of cobalt hydroxide in these bands was calculated and is shown to increase to a maximum away from the interface and then decreases. The bands later grow by further precipitation. This growth was demonstrated to be nonlinear in time. On the other hand, the dissolution of bands was shown to take place simultaneously and collectively among the multiple bands under study. The effect of the concentration of Co^{+2} ions on the dynamics of band formation and dissolution was studied. A time law for this Liesegang system was also determined. The system was also found to be very sensitive to temperature fluctuations.

Introduction

Self-organization in different fields of science is the emergence of macroscopic patterns from local processes and interactions outside equilibrium.[1,2] In chemistry, these patterns result mainly from the coupling of nonlinear chemical reactions with diffusion.[3–5] The emerging patterns can depend on time and exhibit propagating waves, fronts, and spirals,[4] or they can be time-independent and exhibit, for example, Turing patterns.[4] In addition, these nonequilibrium structures might be symmetric or completely chaotic.[6] One classical example of pattern formation in chemistry is the display of spatial oscillations due to periodic precipitation, the so-called Liesegang banding phenomenon,[7,5,8–11] emerging from the coupling of the precipitation reactions with diffusion. When a gel solution, containing a certain electrolyte (called the inner electrolyte), is placed in a test tube with another electrolyte diffusing from its top (the outer electrolyte), a precipitate pattern appears as a set of bands that form parallel to the diffusion front and toward the lower end of the tube. These bands are separated by well-localized precipitate-free zones. Spatial oscillations are thus manifested through the alternation of precipitate in the form of bands or rings and precipitate-free domains. The variation of the conditions under which precipitate patterns are formed and the nature of the chemical reactions taking place reflects on the morphological structure of the pattern, as well as its dynamic properties.[12]

The precipitate bands formed may be static: once formed they maintain their position in space. On the other hand, dynamic precipitate patterns are those in which the formed band might undergo further splitting and dissolution. In a vertical tube, the upper gel portion (close to the interface between the two electrolytes) is more influenced by the excess diffusing electrolyte, which might cause the redissolution of the preformed precipitate bands, whereas at the bottom of the tube precipitate bands persist much longer. A gel containing Co^{2+} displays the green/blue α-$Co(OH)_2$ ($K_{sp} = 3.00 \times 10^{-16}$) bands upon diffusion of NH_4OH, used as the outer electrolyte. α-$Co(OH)_2$ is one of two polymorphs of Cobalt hydroxide.[13] Later, the $Co(OH)_2$ bands near the interface redissolve, forming the orange/yellow $Co(NH_3)_n^{2+}$ complex (for $n = 6$, $K_f = 5.00 \times 10^4$) in excess NH_4OH.[14,15] Thus, new bands are formed at the bottom, and old ones dissolve at the top, and the whole is migrating down the tube. Numerous experimental observations on periodic precipitation patterns with redissolution exist in the literature and include the HgI_2/HgI_4^{2-},[16–19] the $Cr(OH)_3/Cr(OH)_4^-$,[20–22] and the $Al(OH)_3/Al(OH)_4^-$[23] systems. The coupling of diffusion, precipitation, and redissolution governs the dynamics of such migrating Liesegang patterns where complex formation and its effect on periodic precipitation systems by provoking the partial redissolution of the precipitate stimulated a notable interest and was the subject of a number of theoretical modeling investigations.[10,11,24,25] However, most of these experimental studies did not focus on the dynamics of band formation and redissolution and the concomitant studies were based on visual observations which limit the time resolution of the dynamics. By using time-resolved UV−vis spectrophotometry, we were able to address the temporal evolution and study the different parameters affecting the aforementioned patterns in great details.

The effective reaction scheme representing the precipitation and redissolution scenario in the presence of NH_4OH are

$$Co^{+2}(aq) + 2OH^-(aq) \rightarrow \alpha Co(OH)_2(s) \quad (1)$$

$$\alpha Co(OH)_2(s) + nNH_3(l) \rightarrow Co(NH_3)_n^{+2}(aq) + 2OH^-(aq) \quad (2)$$

The ammonium hydroxide used in this study is highly concentrated (13.37 M), and thereby the outer electrolyte

* To whom correspondence should be addressed. E-mail: mazen.ghoul@aub.edu.lb.

10.1021/jp803118r CCC: $40.75
Published on Web 08/09/2008

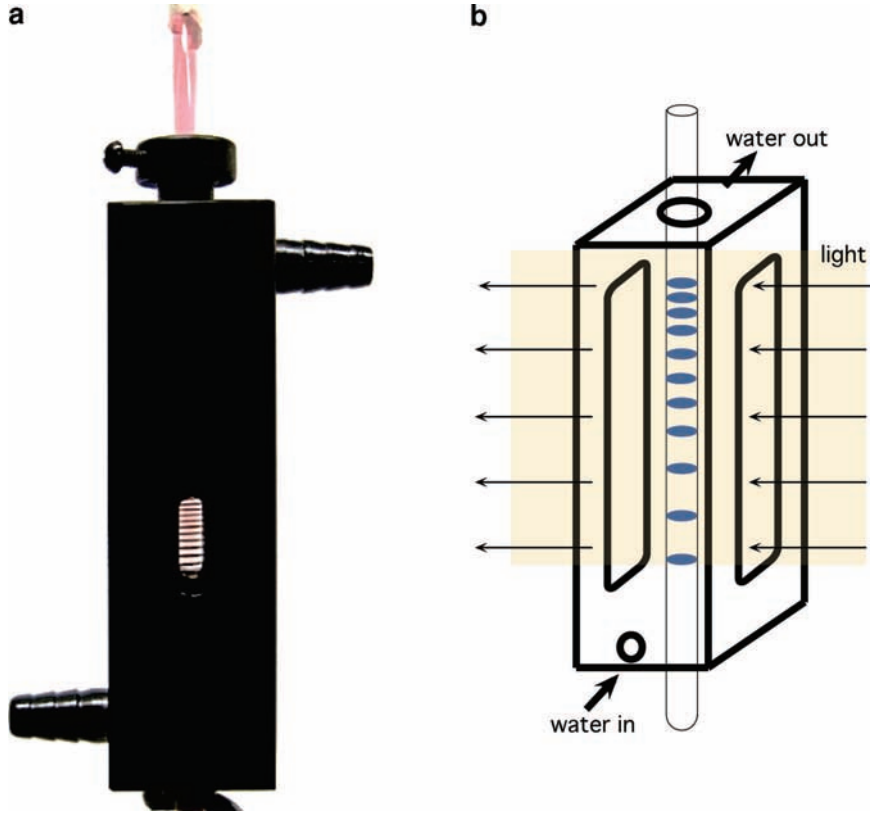

Figure 1. (a) The aluminum sample holder that is designed for the Liesegang experiments. It has the following dimensions: 118.5 × 31 × 30 mm; adjustable open slit 5 × 15 mm; tube hole 6.5 mm. (b) A scheme illustrating the sample (bands in tubes) in the sample holder (Figure 1a) and the light path during the measurments using the spectrophotomemter.

solution contains mainly ammonia (NH_3) and the hydroxide ions (OH^-), which is in a lower concentration because as is well-known ammonia is a weak base in water. The coupling of reactions (1,2) to diffusion in a gel medium will result in the formation and redissolution of Liesegang bands. In this paper, we study the dynamics in this particular system using UV−vis spectroscopy. In what follows, we will first discuss the experimental techniques. Of particular interest is the effect of the initial concentrations of Co^{2+} (cations within the inner electrolyte in gel) on the dynamics. This is presented in section 3. In section 4, we use the technique to study the speed of band formation, dissolution, and composition of the bands. Section 5 contains the determination of a time law. In section 6, we discuss the dissolution regime and nature of the complex. The effect of temperature is discussed in section 7 and in the appendix.

Experimental Section

The required masses of $CoCl_20.6H_2O$ (Fluka) and gelatin (5%) (Difco) are weighed to the nearest 0.0001 g. These masses are then transferred to a beaker containing 5.00 mL of doubly distilled water. After dissolution of the solid, 0.2500 g of gelatin powder are added to make a 5% gelatin solution. The solution is then heated with continuous stirring until all the gelatin dissolves. The resulting gel is immediately transferred using a Pasteur pipet into clean previously prepared test tubes (25 cm long with 0.4 cm diameter) in such a way that each tube is two-thirds full. The tubes are then covered with parafilm paper and allowed to stand for about 24 h in a thermostatic chamber at 18 °C. Before adding the outer electrolyte (NH_4OH solution), the upper edge of the gel is marked to indicate the interface. Then 13.37 M of ammonium hydroxide solution is added to the remaining one-third empty portion of each tube above the solidified Co^{2+}−gel interface. Once the outer electrolyte solution is being added over the interface, a homogeneous greenish blue precipitate starts to form. Photos of the evolution of the tubes are taken with a digital Sony DSC-F717 camera. The tubes are allowed to stand at 18 ° C in an air thermostat for 2−3 h before being analyzed in the UV−vis−NIR spectrophotometer (JASCO V-570 Japan) using a special sample holder (Figure 1) that was specially designed for the experiments reported in this work. This holder is aluminum based with adjustable slit and is designed in order to fit the dimensions of the tubes in which the patterns are being formed. It is also jacketed, and water is allowed to flow in and out and to cycle through a thermostat (Grant LTD6G). Thermostating is essential because the amount of solid cobalt hydroxide in the formed bands is found to be very sensitive even to slight fluctuation in temperature. The temperature is adjusted to 18 °C. To make sure that the effect of temperature fluctuations are minimized, the ambient temperature is recorded every 30 s using a Pasco 750 interface with a temperature sensor. The recorded variation were then compared to the absorbance measurements in order to be validated.

The evolution of the bands is monitored using absorbance at the wavelength corresponding to maximum absorbance for the α-$Co(OH)_2$ precipitate. To determine λ_{max}, we used the KBr pellets technique for the precipitate α-$Co(OH)_2$, which was prepared by the action of a concentrated solution of NH_4OH on a solution of dissolved $CoCl_2.6H_2O$(s). The precipitate is recovered by filtration, washed, and dried. The KBr pellets are then prepared and the absorbance spectrum of the obtained discs was recorded. The maximum absorbance was found to be at 642 nm, and accordingly all experiments in this paper concerning the bands were performed at this wavelength. The choice

of the concentrations of the system was based on previous investigation done by Msharrafieh et al.[30] whereby the experiments are performed in the limit of large initial concentration difference δ ($\delta = {}^1/_2[Co^{2+}]_0 - [NH_4OH]_0$). Therefore, the initial concentration chosen for the outer electrolyte was 13.37 M NH_4OH throughout this work and for the inner electrolyte Co^{2+}, we chose initial concentrations ranging from 0.100 M (assumed as low inner concentration) to 0.600 M (assumed as high inner concentration). For each run, two identical tubes are prepared. One is used for visual observation, and the other is placed in the UV−vis spectrophotometer where absorbance is measured every 1 min. The spectrum is recorded on the computer and saved for further analysis. The size of the slit of the handler can be adjusted depending on the size of the region of the tube where we would like to investigate. The slit can be made as small as to capture up to one band. The experiments were repeated many times to test for reproducibility of the results. Most of the results reported here were reproducible to a satisfactory degree.

Effect of Inner Concentration. In this section, the effect of the inner concentration of Co^{+2} on the dynamics of band formation is investigated. For every initial concentration of the inner electrolyte we tested, we prepared a set of identical samples (gel with the inner electrolyte Co^{+2}) and three types of experiments were performed on these samples: the first type involved absorbance measurements from about an hour after addition of the outer electrolyte until all bands along the open slit of the holder were dissolved. This takes days to be completed. The second type also involved absorbance measurements but the experiments were stopped directly after all bands were formed and before growth or dissolution took place. In the third type, we kept the experiment running in a thermostatted chamber and made visual observations and manual measurements of distances and spacings every hour or so. A typical full-time measurement of absorbance is shown in Figure 3a. In this figure, we can distinguish four different regimes: (1) the prebanding regime which supersedes the formation of the bands; (2) the banding regime where bands start appearing, and this is seen as sudden jumps in the absorbance spectrum; (3) the growth regime which is achieved after all bands within the open slit are formed and get enriched with $Co(OH)_2$; (4) the redissolution of bands regime when the excess ammonia starts dissolving the enriched bands. In Figure 3a, the slit was adjusted to cover a region of the tube a few centimeters away from the interface. All of the following experiments were repeated many times to test for reproducibility. Regimes 1, 2, and 4 were easily reproducible to an excellent degree. However, special care was taken in order to reproduce the growth regime 3 due to extreme sensitivity to temperature fluctuations and to strong dependence on the distance from the interface.

Case of Intermediate Inner Concentration (0.200 M Co^{+2}). We explored visually a whole range of inner concentrations before we started the spectroscopic measurements. It turns out that, in the case where the inner concentration is around 0.200 M Co^{+2}, we are able to obtain the "best" bands in term of resolution and structural stability in the gel medium. The Co^{+2}(aq) is in fact the ion $Co(H_2O)_6^{+2}$, a stable complex with a faint pink color, and was found to have in the gel an absorbance band in the visible region with a maximum absorbance at a wavelength $\lambda = 510$ nm. Figure 2a is the prepared tube with gel containing the Co^{+2} ions. Visually, a few minutes after the addition of NH_4OH, a blue/green sharp band appeared at the interface (Figure 2b), which after a few hours was followed by the appearance of new bands and the dissolution of the former

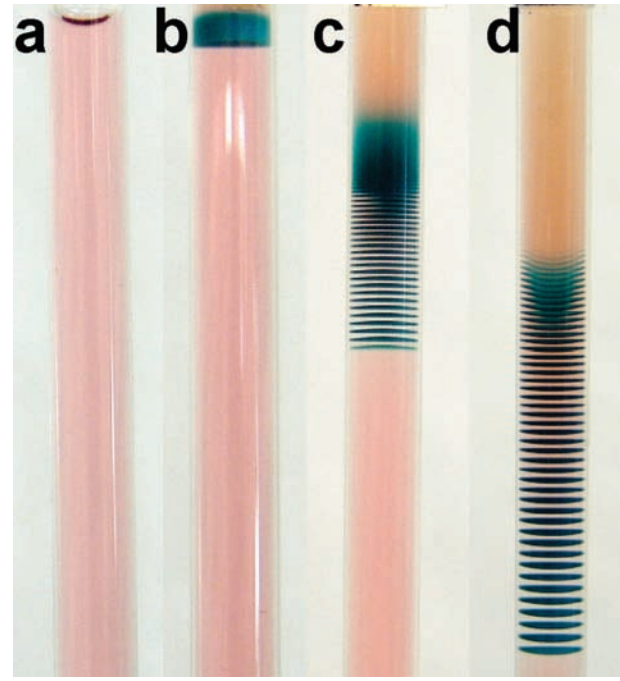

Figure 2. A typical time sequence for a propagating Liesegang pattern for an initial inner concentration of $[Co^{+2}]_0 = 0.2$ M and outer concentration of $[NH_4OH]_0 = 13.37$ M. (a) Gel with with pink-colored Co^{+2}(aq) prior to the addition of the NH_4OH solution; (b) 2 h after the addition of NH_4OH a band of blue-green α-$Co(OH)_2$ forms; (c) one day after the addition of the NH_4OH solution, many bands of α-$Co(OH)_2$ are formed down the tube; (d) 5 days after the addition of the NH_4OH solution, the bands start dissolving near the interface leaving a clear brown/red color due to the formation of $Co(NH_3)_n^{+2}$.

initial band. After two days, we obtained numerous well-resolved bands within the tube (Figure 2c). In subsequent days, the bands on the top started dissolving leaving behind a clear light brown species; this was concomitant with the formation of new bands down the tube (Figure 2d) giving the impression of a propagating stratum down the tube. It is very difficult to obtain information about the dynamics of band formation, growth, and dissolution by mere visual observation. Therefore, we resorted to the spectroscopic technique described earlier to thoroughly study this system. The slit was opened and adjusted in such a way that it starts at the interface and extends downward a few centimeters. In the case corresponding to 0.200 M Co^{+2}, this resulted in a time evolution curve of the absorbance as shown in Figure 3b. The formation of the bands is clearly noticed when the absorbance started exhibiting sudden jumps in the form of sigmoidal curve. Each jump corresponds to the formation of a new band. It is clear that the formation of one band takes about 15 min to half an hour until the next bands starts forming. The inset of Figure 3b represents a zoom on two formed bands. The first band in this inset, delimited between the two dashed vertical lines, started forming at a time of 0.4 days and was completed at a time of 0.45 days, which is about 15 min. After all bands form within the open slot of the handler, we notice an increase of the absorbance as time passes by indicating a growth of these bands by getting enriched with more $Co(OH)_2$ due to a new wave of hydroxide ions that precipitate remaining Co^{+2} ions existing between the bands. The existence of Co^{+2} just after the formation of the bands was directly determined by adjusting the slit of the holder to capture the region between the bands and taking the absorbance spectrum, which reveals a peak at $\lambda = 510$ nm, characteristic of Co^{+2}(aq). The growth of these bands occurred simultaneously as no jumps

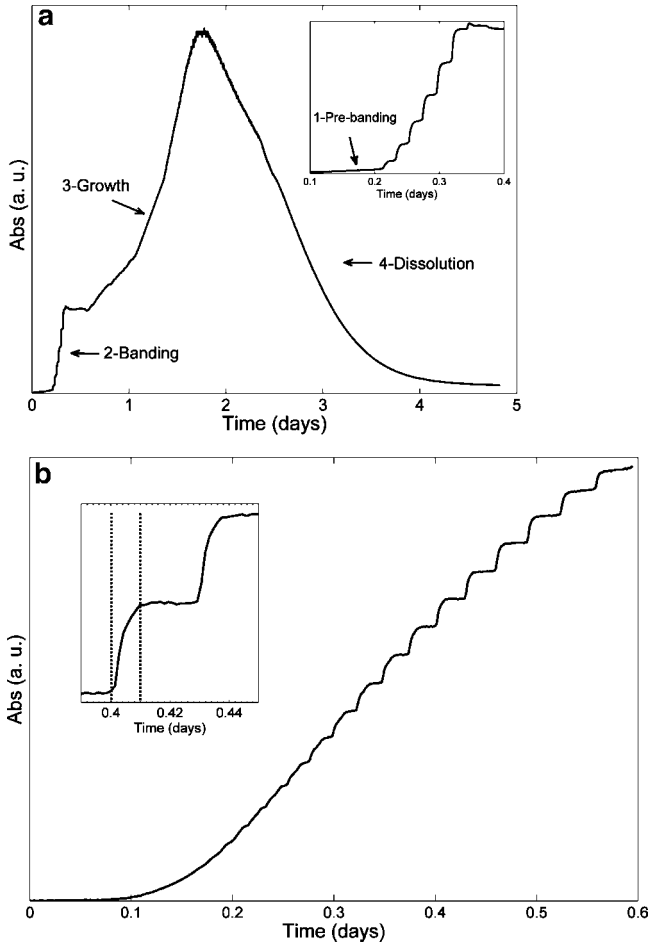

Figure 3. (a) Full-time (days) evolution of absorbance, absorbance in arbitrary units (au), in the case of intermediate inner concentration ($[Co^{2+}]_0 = 0.2$ M) away from the interface. Four different regimes can be distinguished: (1) the prebanding regime, which supersedes the formation of the bands; (2) the banding regime where bands start appearing, and this is seen as sudden jumps in the absorbance spectrum; (3) the growth regime, which is achieved after all bands within the open slit are formed and get enriched with $Co(OH)_2$; (4) the dissolution regime. $[NH_4OH]_0 = 13.37$ M. The inset is a blowup of the banding regime where bands appear as jumps in the absorbance. (b) Time (days) evolution of absorbance in the case of intermediate inner concentration ($[Co^{2+}]_0 = 0.2$ M) near the interface in the prebanding and banding regimes. $[NH_4OH]_0 = 13.37$ M. The inset is a zoom on two formed bands. The first band in this inset is delimited by the 2 dashed horizontal lines located at 0.4 days and 0.45 days and mark the beginning of formation and end of formation of the band.

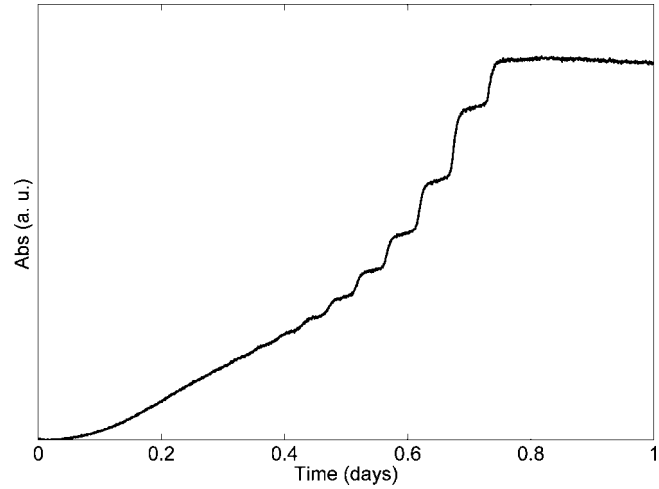

Figure 4. Time (days) evolution of absorbance in the case of low inner concentration ($[Co^{2+}]_0 = 0.1$ M) near the interface in the prebanding and banding regimes. $[NH_4OH]_0 = 13.37$ M.

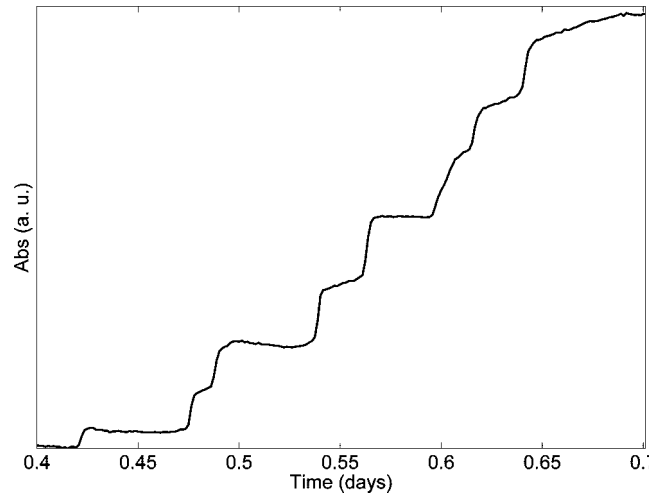

Figure 5. Time (days) evolution of absorbance in the case of high inner concentration ($[Co^{2+}]_0 = 0.6$ M) near the interface in the prebanding and banding regimes. $[NH_4OH]_0 = 13.37$ M.

were seen in this region. This growth continued until the dissolution waves of ammonia had reached the bands which started dissolving. What is noticeable in this region is that the dissolution of the bands did not occur band by band but simultaneously across all bands as reflected by the smooth jump-free profile of the absorbance. The dissolution of the bands proceeded exponentially in time. The nature of the complex formed and the time dynamics of dissolution will be discussed in a section 6. If we move the slit away from the interface to capture some farther bands, the growth seems to be postponed for a period of time proportional to the distance of the slit from the interface, confirming that the growth of the bands is due to a subsequent hydroxide wave that precipitates the excess Co^{+2} ions. This delay can be seen in Figure 3a as a shoulder extending for about 6 h (in this case from time = 0.25−0.5 days).

Case of Low Inner Concentration. In the case of 0.100 M Co^{2+}, which we consider as low inner concentration, a few minutes after the addition of NH_4OH, a continuous green haze of α-$Co(OH)_2$ started forming near the interface and extends a few centimeters below (Figure 4). This is clearly seen in the relatively long span in time (about half a day) of absorbance before jumps occurred, i.e., before banding started occurring. This increase in the absorbance due to formation of the continuous haze region is nonlinear in time. After a few hours, the haze divides into bands. After two days, we obtain a few well-resolved bands with a steplike appearance in the time evolution of the absorbance.

Case of High Inner Concentration. Above 0.600 M Co^{+2} the bands where not structurally stable and start breaking shortly after they form. Therefore, this case roughly marks the limit, beyond which no well-resolved Liesegang bands are possible. This structural instability can also be captured by this proposed spectroscopic technique. In Figure 5, in the case of 0.600 M Co^{+2}, we can see the erratic behavior of the absorbance during the formation of the bands. There is also a nonlinear growth of the bands after they form within the open slot. After this regime, the dissolution of the formed bands starts taking place until all are dissolved. The dissolution also proceeds exponentially in time.

Speed of Band Formation and Relative Composition. To shed more light on the dynamics of band formation, the speed

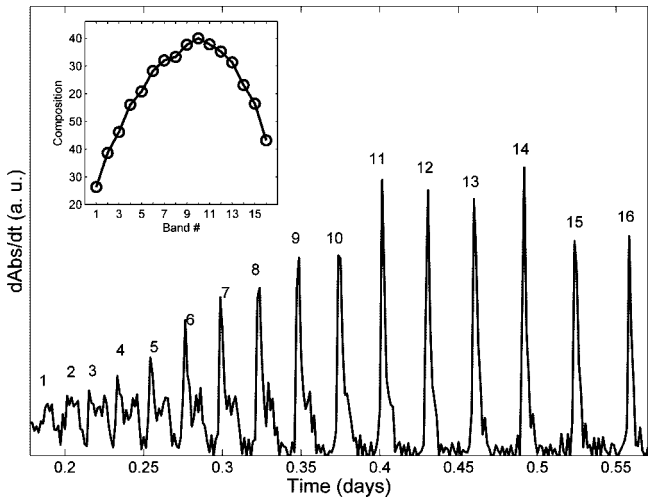

Figure 6. Speed of formation of the bands vs time in the case $[Co^{+2}]_0 = 0.2$ M and $[NH_4OH]_0 = 13.37$ M. The captured bands are numbered. The inset in Figure 6 is a plot of the relative composition of $Co(OH)_2$ contained in the 16 captured bands.

of formation of the bands is computed by taking the time derivative of the absorbance during the formation of the bands. In the case of 0.200 M Co^{+2}, the results are shown in Figure 6. In this figure, 16 successive bands were able to be captured and are numbered. Each jump in the absorbance is now a spike in this representation. This means that there is an inflection point in terms of speed as the band forms: it starts forming at increasing speeds, reaches a maximum, and then slows down until the next band forms. It is noticeable that the maximum speeds of formation of the consecutive bands under study are are neither constant nor monotonic but fit a Gaussian-like distribution. It is also noticeable that the maxima of speeds does not exhibit an increasing trend but some stochasticity as clearly shown in Figure 6 where, for example, the maximum speed of band 10 is less than that of band 11; it then decreases in bands 12 and 13 and increases for band 14 to decrease again in band 15 and 16. This type of random fluctuations in no strange in the Liesegang phenomena[31] and is not well-understood. The time-spacing between the spikes is not constant and increases with time confirming the spacing law in the Liesegang experiment, i.e., the spacing between the consecutive bands increases as the bands move down the tube.

The bands through the whole pattern maintain their spatial location and do not move until they are dissolved. However, during the pattern evolution, each band undergoes a change of its $Co(OH)_2$ mass composition. The mass of $Co(OH)_2$ in a given band was determined by time integration between the edges of the corresponding peak in the speed of band formation vs time curve shown in Figure 6. The inset in Figure 6 is a plot of the relative composition of $Co(OH)_2$ contained in the 16 captured bands, with $[Co^{2+}]_0 = 0.200$ M, as a function of band numbers during the coarse of their formation within the open slit of the sample holder. It is noticed that the bands that contain most of precipitate are not the closest to the interface but are those that are approximately in the middle, namely, those around the 10th band. In other words, the mass of the precipitate starts increasing as we move from bands close to the interface toward the bottom of the tube, reaches a maximum, and then starts decreasing. This switch in the trend is interesting and reveals a competition scenario between precipitation and dissolution as early as the formation of the first bands: The hydroxide ions increase the amount of precipitate, and the ammonia decreases it by dissolving it to form the complex. This can also be confirmed

TABLE 1: Time Law Expressed in Terms of the Constants α and *p* for the Four Separate Experiments I, II, III, and IV Where the Inner Concentration Is Varried[a]

exp no.	$[Co^{2+}]_0$ (M)	$[NH_4^+]_0$ (M)	δ	π	α	r_∞	*p*
I	0.22	13.37	6.575	2.941	0.0383	1.04	0.04
II	0.25	13.37	6.560	3.343	0.057	1.06	0.06
III	0.30	13.37	6.535	4.011	0.090	1.09	0.09
IV	0.4	13.37	6.485	5.348	0.317	1.1	0.1

[a] r_∞ is an approximate value estimated in the limit of large *n*.

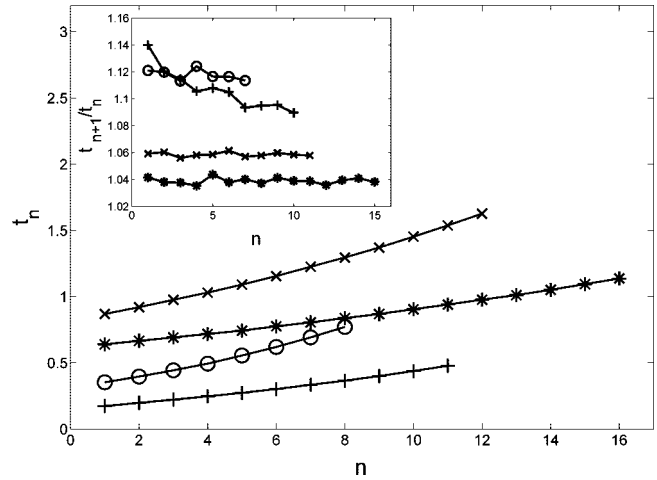

Figure 7. Time at which the *n*th band starts forming, t_n vs the band number *n*: ∗, I; ×, II; +, III; ○, IV. The inset shows the plot of r_n vs *n* for experiments I, II, III, and IV.

by taking the UV−vis spectrum of the material in the tube close to the interface which reveals the formation of a considerable amount of the cobalt−amine complex near the interface and a less amount of this complex between the bands away from the interface. As the NH_4OH concentration starts to decrease after this maximum (diffusion profile smoothens), which also means that both the hydroxide ions and ammonia start decreasing, less cobalt hydroxide is precipitated and at the same time ammonia is also insufficient for the effective dissolution of cobalt hydroxide. Similar behavior was observed in a study on a two-salt Liesegang system.[31] On theoretical aspects, using two separate models[24,25,10,31] describing Liesegang systems with precipitation/redissolution, the mass of precipitate was found to increase within the bands as the latter move away from the junction. The role of the complex formation in related experiments was recently investigated by Badr and Sultan.[32] They found that, although the complex profiles were not conjectured and plotted in those aforementioned theoretical studies, the spatial distribution of the complex ion concentration essentially reproduces the behavior observed here, since the amounts of precipitate and complex were anticorrelated.

Time Law. As we saw in previous sections, this developed technique can be used to accurately determine the temporal dynamics of band formation and furthermore, it allows us to derive a time law for this Liesegang system. We prepared four different experiments where we kept the outer concentration of NH_4OH fixed at 13.37 M and varied the inner concentration of Co^{2+} as illustrated in Table 1. By use of the speed of the bands vs time plot for these experiments, we were able to determine the time at which the *n*th band starts forming and is denoted as t_n. t_n is then plotted as a function of *n* and the results were depicted in Figure 7. The dependence of t_n on *n* was found to perfectly fit an exponential of the form $t_n \approx \exp(\alpha n)$ where α is a constant that depends on the initial concentration product

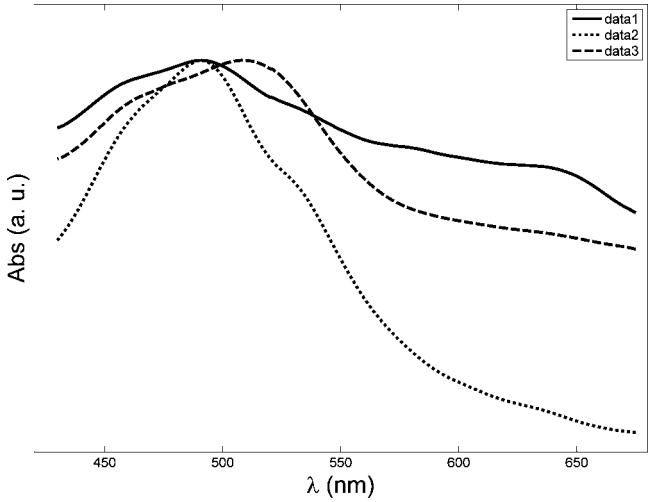

Figure 8. UV−vis spectra, absorbance vs wavelength λ, of the different species present after redissolution of the bands near the interface. $[Co^{+2}]_0 = 0.2$ M and $[NH_4OH\ ]_0 = 13.37$ M. The dashed curve is the spectrum taken when the slit was adjusted in the clear region below the bands. The peak at 510 nm and the shoulder at 463 nm confirms the presence of only the ion $Co(H_2O)_6^{+2}$. The dotted curve is the spectrum taken for the dissolved bands region near the interface. The peak at 491 nm and the shoulders at 460 and 531 nm indicate that the species present is the complex $Co(NH_3)_n^{2+}$ $(1 \le n \le 6)$. The solid line is the spectrum taken in a region where we have bands. The peaks at 458, 491, and 531 nm indicate the presence of $Co(H_2O)_6^{+2}$ and $Co(NH_3)_n^{2+}$, and the band at 641 nm is specific to $Co(OH)_2$ (s).

π. This constant α is found to increase with increasing π as shown in Table 1. To obtain a time law, we define r_n as the ratio of consecutive t_n values, i.e., $r_n = t_{n+1}/t_n$. The plot of r_n as a function of n is shown to tend to a constant close to 1 in the limit of large band number n. The inset in Figure 7 exhibits such a result. We can recast r_n as

$$r_n = \frac{t_{n+1}}{t_n} \approx 1 + p \tag{3}$$

where p is a constant in the limit of large n. We found that p increase as π increases and the results are shown in table

Dissolution Regime. The dissolution of the uppermost bands of $Co(OH)_2$ took place after a few days of their formation. As the dissolution proceeds, more bands form down the tube. When the solid dissolves, a yellow/orange clear gel is left indicating the presence of a complex. To explore this regime, we adjusted the position of tube in the sample holder so that the dissolution region can be explored spectroscopically and the UV−vis spectrum of this clear region can be measured. The corresponding spectrum is shown in Figure 8. The colored ion is identified as a possible mixture of $Co(NH_3)_n^{+2}$ $(1 \le n \le 6)$. It is identified as such because of the presence of a maximum at $\lambda = 490$ nm and the shoulder at $\lambda = 530$ nm. The latter shoulder is what characterizes the ammine complexes of Co(II) ions. This existence of a mixture is probably due to the close values of the formation constants β_n for $3 \le n \le 6$. These formation constants for the complexes $Co(NH_3)_n^{+2}$ $(1 \le n \le 6)$ are, at 30 °C and zero ionic strength, $\log \beta_1 = 1.99$, $\log \beta_2 = 3.50$, $\log \beta_3 = 4.43$, $\log \beta_4 = 5.07$, $\log \beta_5 = 5.13$, $\log \beta_6 = 4.39$, respectively.[26] Although the temperature at which the experiments were carried was 18 °C, the aforementioned formation constants can still be used for a relative comparison. It might also be that the gel has slowed down the substitution reactions between the chloride ions and the carbonate ions with the water on the hydrated Co^{+2} centers since there is no indication in the spectrum of the existence chloro or carbonato Co(II) complexes; an opposite behavior is obtained when for example $CoCl_2$(aq) is treated with excess ammonia. in such a case, a mixture of different ammonia complexes are thus obtained and consequently no clear spectrum can be obtained. We also found no evidence of any Co(III) ammine complexes such as $Co(NH_3)_n^{+3}$ (for $n = 6$, $K_f \approx 10^{34}$), which usually exhibit two maxima between 400 and 600 nm, which implies that the gel has apparently stabilized the Co(II) complex by preventing oxygen from oxidizing it to Co(III), something that could have easily happened in water and this a well-known fact about the ammine complexes of cobalt(II).[27–29]

TABLE 2: Variation of the Exponent κ for the Three Different Experiments I, II, and III for Different Inner Concentrations

exp no.	$[Co^{2+}]_0$ (M)	$[NH_4^+]_0$ (M)	δ	κ
I	0.20	13.37	6.585	1.744
II	0.30	13.37	6.535	1.233
III	0.60	13.37	6.385	0.861

When a new front carrying the excess ammonia arrive at the bands, it starts reacting with the solid $Co(OH)_2$, which in turn dissolves leaving behind the aforementioned complexes. The first thing noticeable is that the dissolution occurs in a continuous and smooth manner opposite to what is observed during the formation of the bands. This means that the bands start dissolving in groups and not individually. By use of the time evolution curves of absorbance in the dissolution regime, we can study the dynamics of dissolution as a function of the inner concentration and time. We were able to fit the drop in absorbance due to the dissolution of bands to an exponential, and the fit was excellent. Therefore, in this regime, the absorbance, abs, was found to depend on time as

$$\text{Abs} \approx \exp(-\kappa t) \tag{4}$$

where t is time and κ is a rate constant characterizing the speed of dissolution. We found that κ increases as δ increases. Table 2 summarizes this.

Many theoretical models[24,25,10,11,31] were used to study the redissolution of bands, but none of these models studied the kinetics of the redissolution in the way it approached in this work, i.e. no functional dependence on time similar to eq 4 was obtained. However, in the model by Lagzi[24] where the outer electrolyte invades a gel medium containing an inner electrolyte of uniform distribution coupled to a CSTR, some aspects of the dynamics of redissolution by complex formation was studied.

Temperature Dependence. The Liesegang system studied in this paper was found to be very sensitive to temperature fluctuations. We noticed at the beginning of our experiments that there were about 4−6 °C around an ambient temperature of about 22 °C in the laboratory space where the absorbance measurements were carried. The temperature was periodic of periods ranging from 4 to 8 h depending on the time of the week and year. We have recorded all temperature variation during all the measurements in this work using a Pasco 750 Interface with a temperature sensor inserted in the spectrophotometer near the sample holder. The temperature recording was done every 5 min. To study the effect of temperature on the dynamics of bands in the system understudy, we turned off the thermostat after the bands have formed within the open slit of the sample holder and recorded the absorbance. A perfect correlation between the variation of absorbance and that of the temperature is depicted in Figure 9. As temperature increases, absorbance decreases due to the decrease in the concentration

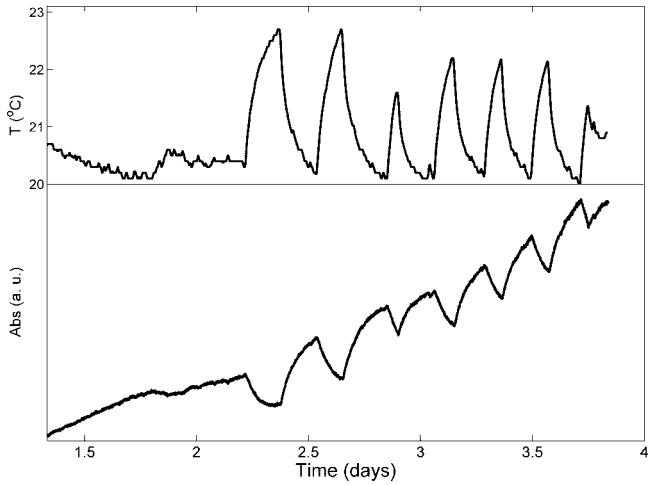

Figure 9. Plots of absorbance, abs (au), (lower curve) and temperature, T, (upper curve) as a function time for $[Co^{+2}]_0 = 0.22$ M and $[NH_4OH]_0 = 13.37$ M.

of the precipitate $Co(OH)_2$ since the reaction of precipitation was found to be exothermic. A change of about 4 °C in temperature was reflected in a change of about 20% in the absorbance. Calculation of the change of solubility (appendix) as a function of temperature gives a qualitative agreement with the observed results. Furthermore, the response to temperature fluctuation by the Liesegang system was immediate without any lag. Therefore, it is very important to insulate the system from even the slightest variation in temperature if quantitative analysis is to be performed on the Liesegang bands. Such a caution, we believe, should be taken when experiments involving quantitative analysis of any Liesegang system are to be carried. This sensitive dependence on temperature asserts the kinetic rather than the thermodynamic nature of the chemical processes in the Liesegang system.

Conclusion

The present study unravels a great deal of information about the temporal dynamics of the $Co(OH)_2/NH_4$ OH Liesegang system. The emergent complexity of the dynamics in such a system originates from the chemical complex formation which triggers redissolution and thus adds to the diversity of the chemical processes. The temporal dynamics are studied with a spectroscopic technique where the evolution of the absorbance in the visible region of the spectrum is measured. This method allows accurate determination of the temporal dynamics of band formation due to precipitation, growth, and dissolution due to complex formation. We showed that using this method we can study the composition of the bands and identify all compounds present at any location of the tube. We were able to formulate a time law and found the ratio of the time of formation of consecutive bands tend to a constant close to 1. As for the dissolution, we found the that it is exponential in time and first order in the concentration of the inner electrolyte. We also found that this system is very sensitive to temperature fluctuations.

In the future, we will be focusing on two fronts: the theoretical modeling and the temperature effects. The modeling combines both nucleation and kinetics of particle growth, coupled to diffusion. We have also started applying this techniques to the two-salt Liesegang system $Ni(OH)_2/Co(OH)_2$ with redissolution. We will also like to use this techniques to study the dynamics of formation and competition of the two polymorphs α and β of $Co(OH)_2$, which are obtained when Co^{+2} are treated with a strong base like NaOH.

TABLE 3: Different Reactions and Corresponding Thermodynamic Properties

reaction	ΔH_f^0 (kJ/mol)	ΔG_f^0 (kJ/mol)
$Co(s) \rightarrow Co^{2+}(aq)$	−58.2	−54.4
$^1/_2H_2(g) + {}^1/_2O_2(g) \rightarrow OH^-(aq)$	−230	−157.2
$Co(s) + H_2(g) + O_2(g) \rightarrow Co(OH)_2(s)$	−539.7	−454.3

TABLE 4: Different Ions Present in the Gel and Their Corresponding Diameter and Estimated Concentrations

ions	diameter r_i (Å)	concentration c_i (M)
Co^{2+}	6	0.2
NH_4^+	2.5	0.0155
Cl^-	3	0.2
OH^-	3.5	0.0155

Appendix

In this appendix, we would like to calculate the various thermodynamic quantities pertaining to the precipitation reaction of cobalt hydroxide. We will then use these quantities to calculate the dependence of the solubility of cobalt hydroxide on temperature. The precipitation reaction is given by the following chemical reaction

$$Co^{2+}(aq) + 2OH^-(aq) \rightarrow Co(OH)_2(s) \quad (5)$$

To calculate the thermodynamics of this reaction, we resort to the following reactions tabulated in table 1 with their ΔH_f^0 and ΔG_f^0, now shown in Table 3.

By use of these reactions, we find for eq 5 $\Delta H^0 = -21.5$ kJ/mol and $\Delta G^0 = -85.5$ kJ/mol.

The dissolution reaction for $Co(OH)_2$ (s) is given by

$$Co(OH)_2(s) \rightleftharpoons Co^{2+}(aq) + 2OH^-(aq) \quad (6)$$

The solubility product K_{sp} for this reaction is given by

$$K_{sp} = aCo^{+2} \times a_{OH^-}^2 = 4\gamma + \gamma_-^2 s^3 = \exp\left(-\frac{\Delta G^0}{RT}\right) \quad (7)$$

where $a_{Co^{+2}}$ and a_{OH^-} are the activities of Co^{+2} and OH^-, s is the solubility, and γ_+ and γ_- are the activity coefficients of Co^{+2} and OH^- ions, respectively. The dependence of the solubility s on temperature can then be deduced from eq 7 as

$$s = \left[\frac{\exp\left(-\frac{\Delta G^0}{RT}\right)}{4\gamma_+\gamma_-^2}\right]^{1/3} \quad (8)$$

The coefficients γ_+ and γ_- are calculated according to the following equation

$$-\log \gamma_i = \frac{Az^2 I^{1/2}}{1 + r_i B I^{1/2}} \quad (9)$$

where I is the ionic strength and is equal to $^1/_2 \sum_i z_i^2 c_i$ where z_i, c_i, and r_i are the charge, concentration, and radius of the ion i, respectively. A and B are functions of temperature and given by $A = 9.0 \times 10^{-4}T + 0.4868$ and $B = 2.0 \times 10^{-4}T + 0.0.3241$. By use of Tables 3 and 4 and eq 7, we obtain the dependence of the solubility on temperature. For example, the ration of $s(t = 23\ °C)/s(t = 20\ °C)$ is found to be equal to 0.896.

Acknowledgment. The authors thank Profs. Tarek Ghaddar, Houssam El-Rassy, and Rabih Sultan for valuable discussions.

The authors would like to acknowledge the support of a grant from the University Research Board, American University of Beirut.

References and Notes

(1) Cross, M. C.; Hohenberg, P. C. *Rev. Mod. Phys.* **1993**, *65*, 851–1112.
(2) Murray, J. D. *Mathematical Biology I*; Springer: New York, 2002.
(3) Pojman, J. A.; Epstein, I. R. *An Introduction to Nonlinear Chemical Dynamics*; Oxford University Press: Oxford, 1998.
(4) Kapral, R.; Showalter, K. *Chemical Waves and Patterns*; Kluwer Academic Publishers: Dodrencht, 1995.
(5) Ball, P. *The Self-Made Tapestry: Pattern Formation in Nature*; Oxford University Press: Oxford, 1999.
(6) Stern, K. H. *Chem. Rev.* **1954**, *54*, 79.
(7) For a nice overview of the Liesegang phenomenon: http://www.insilico.hu/liesegang/index.html.
(8) Liesegang, R. E. *Chem. Fernwirkung. Lieseg. Photograph. Arch.* **1896**, *37*, 305.
(9) Henisch, H. *Crystals in Gels and Liesegang Rings*; Cambridge University Press: Cambridge, 1988.
(10) Al-Ghoul, M.; Sultan, R. *J. Phys. Chem. A* **2001**, *105*, 8053–8058.
(11) Al-Ghoul, M.; Sultan, R. *J. Phys. Chem. A* **2003**, *107*, 8053–8058.
(12) Shreif, Z.; Mandalian, L.; Abi-Haydar, A.; Sultan, R. *Phys. Chem. Chem. Phys.* **2004**, *6*, 3461.
(13) Batlouni, H.; El-Rassy, H.; Al-Ghoul, M. *Inorg. Chem.*, submitted.
(14) Nasreddine, V.; Sultan, R. *J. Phys. Chem. A* **1999**, *103*, 2934.
(15) Lloyd, F. E.; Moravek, V. *Plant Physiol.* **1928**, *3*, 101.
(16) Das, I.; Pushkarna, A.; Argawal, N. R. *J. Phys. Chem.* **1987**, *91*, 747.
(17) Das, I.; Pushkarna, A.; Argawal, N. R. *J. Phys. Chem.* **1989**, *93*, 7269.
(18) Das, I.; Pushkarna, A.; Bhattacharjee, A. *J. Phys. Chem.* **1990**, *94*, 8968.
(19) Das, I.; Pushkarna, A.; Bhattacharjee, A. *J. Phys. Chem.* **1991**, *95*, 3866.
(20) Zrîyi, M.; Gálfi, L.; Smidróczki, É.; Rácz, Z.; Horkay, F. *J. Phys. Chem.* **1991**, *95*, 1618.
(21) Sultan, R.; Panjarian, S. H. *Physica D* **2001**, *157*, 241.
(22) Hilal, N.; Sultan, R. *Chem. Phys. Lett.* **2003**, *373*, 183.
(23) Volford, A.; Izsak, F.; Ripszam, M.; Lagzi, I. *J. Phys. Chem. B* **2006**, *110*, 4535.
(24) Lagzi, I. *J. Phys. Chem. B* **2003**, *107*, 13750–13753.
(25) Izsák, F.; Lagzi, I. *J. Phys. Chem. A* **2005**, *109*, 730–733.
(26) Harris, D. *Quantitative Chemical Analysis*, 7th ed.; Freeman: New York, 2007.
(27) Douglas, B.; McDanieal, D.; Alexnader, J. *Concepts and Models of Inorganic Chemistry*, 3rd ed.; Wiley: New York, 1994.
(28) Attieh, M.; Al-Kassem, N.; Sultan, R. *J. Chem. Soc., Faraday Transactions* **1998**, *194*, 2187–2194.
(29) Sultan, R.; Al-Kassem, N.; Sultan, A. A-H.; Salem, N. *Phys. Chem. Chem. Phys.* **2000**, *2*, 3155–3162.
(30) Al-Msharrafieh, M. M.Sc. Thesis, American University of Beirut, Beirut, 2004.
(31) Msharrafieh, M.; Al-Ghoul, M.; Batlouni, H.; Sultan, R. *J. Phys. Chem. A* **2007**, *111*, 6967–6976.
(32) Badr, L.; Sultan, R. *Chem. Phys. Lett.* **2008**, *453*, 40.

JP803118R